



Comparative cellular toxicity of titanium dioxide nanoparticles on human astrocyte and neuronal cells after acute and prolonged exposure



Teresa Coccini ^{a,*}, Stefania Grandi ^b, Davide Lonati ^a, Carlo Locatelli ^a, Uliana De Simone ^a

^a Laboratory of Clinical & Experimental Toxicology and Poison Control Center, Toxicology Unit, IRCCS Salvatore Maugeri Foundation and University of Pavia, Pavia, Italy

^b N.A.M Srl, NANO-Analysis & Materials, Pavia, Italy

ARTICLE INFO

Article history:

Received 3 November 2014

Accepted 7 March 2015

Available online 14 March 2015

Keywords:

Neurotoxicity

SH-SY5Y cells

D384 cells

In vitro

Nanomaterials

Safety

ABSTRACT

Although in the last few decades, titanium dioxide nanoparticles (TiO₂NPs) have attracted extensive interest due to their use in wide range of applications, their influences on human health are still quite uncertain and less known. Evidence exists indicating TiO₂NPs ability to enter the brain, thus representing a realistic risk factor for both chronic and accidental exposure with the consequent needs for more detailed investigation on CNS.

A rapid and effective *in vitro* test strategy has been applied to determine the effects of TiO₂NPs anatase isoform, on human glial (D384) and neuronal (SH-SY5Y) cell lines. Toxicity was assessed at different levels: mitochondrial function (by MTT), membrane integrity and cell morphology (by calcein AM/PI staining) after acute exposure (4–24–48 h) at doses from 1.5 to 250 µg/ml as well as growth and cell proliferation (by clonogenic test) after prolonged exposure (7–10 days) at sub-toxic concentrations (from 0.05 to 31 µg/ml). The cytotoxic effects of TiO₂NPs were compared with those caused by TiO₂ bulk counterpart treatment.

Acute TiO₂NP exposure produced (i) dose- and time-dependent alterations of the mitochondrial function on D384 and SH-SY5Y cells starting at 31 and 15 µg/ml doses, respectively, after 24 h exposure. SH-SY5Y were slightly more sensitive than D384 cells; and (ii) cell membrane damage occurring at 125 µg/ml after 24 h exposure in both cerebral cells. Comparatively, the effects of TiO₂ bulk were less pronounced than those induced by nanoparticles in both cerebral cell lines.

Prolonged exposure indicated that the proliferative capacity (colony size) was compromised at the extremely low TiO₂NP doses namely 1.5 µg/ml and 0.1 µg/ml for D384 and SH-SY5Y, respectively; cell sensitivity was still higher for SH-SY5Y compared to D384. Colony number decrease (15%) was also evidenced at ≥0.2 µg/ml TiO₂NP dose. Whereas, TiO₂ bulk treatment affected cell morphology only.

TiO₂ internalization in SH-SY5Y and D384 cells was appreciated using light microscopy.

These findings indicated, that (i) human cerebral SH-SY5Y and D384 cell lines exposed to TiO₂NPs were affected not only after acute but even after prolonged exposure at particularly low doses (≥0.1 µg/ml), (ii) these *in vitro* critical doses were comparable to literature brain Ti levels detected in lab animal intranasally administered with TiO₂NP and associated to neurotoxic effects.

In summary, the applied cell-based screening platform seems to provide effective means to initial evaluation of TiO₂NP toxicity on CNS.

© 2015 Elsevier Inc. All rights reserved.

1. Introduction

Titanium dioxide (TiO₂) is a versatile compound that has broadly been used in nanoparticles form, titanium dioxide

nanoparticles (TiO₂NPs). According to the U.S. National Nanotechnology Initiative, they are one the most highly manufactured in the world due to their high physical stability, anticorrosion and photocatalytic activity (Baan et al., 2006; Shi et al., 2013). TiO₂NPs are in the top five NPs used in consumer products (Shukla et al., 2011), widely used in paints, printing ink, rubber, paper, car materials, cleaning air products, sterilization (Montazer and Seifollahzadeh, 2011), industrial photocatalytic processes (Douglas et al., 2000), decomposing organic matters in wastewater

* Corresponding author at: Laboratory of Clinical & Experimental Toxicology, IRCCS Salvatore Maugeri Foundation, Institute of Pavia, Via Maugeri 10, 27100 Pavia, Italy. Tel.: +39 0382 592416; fax: +39 0382 24605.

E-mail address: teresa.coccini@fsm.it (T. Coccini).

(Sun et al., 2004) and as an additive in cosmetics (Kaida et al., 2004; Wolf et al., 2003), pharmaceuticals, and food colorants (Jin et al., 2008; Vamanu et al., 2008a).

Human exposure to TiO₂NPs may occur during both manufacturing and use. TiO₂NPs can be encountered as aerosols, suspensions or emulsions. The major route of TiO₂NP exposure that have toxicological relevance in the workplace is inhalation.

The United States National Institute for Occupational Safety and Health (NIOSH, 2011) proposed a recommended exposure limit (REL) for TiO₂NPs at 0.3 mg/m³, which was 10 times lower than the REL for TiO₂FPs (FP: fine particles). Despite TiO₂NPs have been regulated, there are still many concerns related to their small size and their potential toxic effects after inhalation.

Human data related to absorption through inhalation of TiO₂NPs are currently not available. Numerous pulmonary rodent studies were carried out to clarify the role played of TiO₂NPs in determining lung injury after acute or chronic exposure (Bermudez et al., 2004; Grassian et al., 2007; Kobayashi et al., 2009; Li et al., 2010; Ma-Hock et al., 2009; Osier and Oberdörster, 1997; Sun et al., 2012; Tang et al., 2011; Warheit et al., 2007a,b; Ze et al., 2014a,b). Several studies have also reported that, irrespective of the route of exposure, TiO₂NPs enter systemic circulation and migrate to various organs and tissues including brain where they could accumulate and cause damage (e.g., structural changes in the neuronal architecture, changes in the release and metabolism of neurotransmitters) (Hu et al., 2010; Kreyling et al., 2002; Li et al., 2010; Ma et al., 2010; Oberdörster et al., 2009; Takenaka et al., 2001; Wang et al., 2007, 2008a,b; Ze et al., 2014a,b).

Currently, *in vitro* cellular studies regarding the molecular mechanism of the neurotoxicity and the effects of TiO₂NPs (pure anatase isoform or anatase/rutile mixture) on the nervous system are scarce and limited to rat neuronal (PC12, N27), murine glial cell lines (C6, BV-2, N9), primary neural cells obtained from rodents (Huerta-García et al., 2014; Liu et al., 2010; Long et al., 2006, 2007; Márquez-Ramírez et al., 2012; XiaoBo et al., 2009; Wu et al., 2010), or *in vitro* cell-based rat blood–brain model (Brun et al., 2012) after acute TiO₂NPs exposure. Few studies have been focused on neurotoxicity of TiO₂NPs in human nervous system cells (e.g. SH-SY5Y, U373, U87) and in any way after acute exposure only (Huerta-García et al., 2014; Lai et al., 2008; Valdiglesias et al., 2013).

Understanding the health impact of TiO₂NPs has become a priority both for ensuring health protection and for regulating the safe development of nanotechnologies. The ability of TiO₂NPs to enter the brain represents a realistic risk factor both in the case of chronic and accidental exposure, which needs to be investigated in more detail.

In vitro human cell models may represent a valid instrument to investigate TiO₂NP effects on CNS and to determine their underlying mechanistic processes, providing information about doses of exposure. Thus, to fulfill the goal of facilitating predictions of toxicological profiles and improve human risk assessment by using *in vitro* data (Westerink, 2013), a rapid and effective *in vitro* test strategy has been applied allowing to meet some basic requirements, including a relevant exposure paradigm (e.g., prolonged exposure to low concentrations), relevant endpoint(s) and cell models (e.g., both neuronal and glial cells) to match the neurotoxic evaluation question.

In this respect, the present study aimed at determining the effects of TiO₂NPs anatase isoform, on human glial cells (D384 cell line) and neuronal cells (SH-SY5Y cell line). Toxicity was assessed at different levels: mitochondrial function, membrane integrity and cell morphology after acute exposure (4–48 h) at doses ranging from 1.5 to 250 µg/ml as well as growth and cell proliferation after prolonged exposure (7–10 days) at doses

ranging from 0.05 to 31 µg/ml. The cytotoxic effects of TiO₂NPs were compared with those caused by treatment with TiO₂ bulk counterpart.

2. Materials and methods

2.1. Chemicals

All reagents and chemicals for cell cultures, Titanium (IV) oxide (TiO₂), and chemicals for light microscopy analyses were purchased from Sigma–Aldrich (Milan, Italy).

2.2. Physico-chemical characterization of TiO₂NP

Titanium oxide nanoparticles (# 5430MR) were purchased from Nanostructured & Amorphous Materials, Inc. (Houston, USA). The presence of TiO₂ was confirmed by X-ray diffraction analysis (Fig. 1A, data provided by the Company). The TiO₂NP nanopowder, anatase isoform, presented spherical form, primary particle size of 15 nm, specific surface area of 240 m²/g, density of 3.9 g/cm³, purity of 99.6%. Metal impurities evaluated by inductively coupled plasma were: Na 0.01%, Fe 0.004%, Mg 0.006%, Al 0.01% and Cl 0.01%. Further evaluations by morpho-dimensional analysis of the raw nanomaterial in water by TEM and SEM (Fig. 1B1 and B2) and dynamic light scattering (DLS) indicated a diameter size of 69.3 ± 0.4 nm.

Moreover, the size of the nanoparticles and the zeta potential in the stock suspension and culture media were analyzed by dynamic light scattering (DLS) using the Malvern Zetasizer Nano ZS90. For these measurements, TiO₂NP were prepared using the dispersion protocol indicated below (Section 2.4) and diluted in the culture media for the two cell line treatments. Specifically, the evaluations were performed in stock solution (TiO₂NP: 2.5 mg/ml), and in completed DMEM and Ham's F12 media (as indicated in Section 2.3) (TiO₂NP: 31 µg/ml) after 24 and 48 h.

2.3. Cell lines

Human neuroblastoma (SH-SY5Y cell line purchased from ECACC, Sigma–Aldrich, Milan, Italy), and human astrocytoma cells (D384 clonal cell line was established from Balmforth et al., 1986), were used for *in vitro* studies of the TiO₂NP and TiO₂ bulk toxicity after acute (4–48 h) and prolonged (7–10 days) exposure.

SH-SY5Y cells were cultured in Eagle's minimum essential medium and Ham's F12 (1:1) with 15% fetal bovine serum (FBS), 2 mM L-glutamine, 50 IU/ml penicillin, and 50 µg/ml streptomycin. D384 cells were cultured in Dulbecco's modified Eagle medium (DMEM) supplemented with 10% FBS, 2 mM L-glutamine, 50 IU/ml penicillin, 50 µg/ml streptomycin and 1% sodium pyruvate. Cells were maintained at 37 °C in a humidified atmosphere (95% air/5% CO₂).

2.4. TiO₂NP and TiO₂ bulk stock suspension

For cell treatments in culture medium, we adopted an optimized dispersion protocol to yield stable stock suspensions of TiO₂NP at pH 7. Specifically, TiO₂NP suspension was prepared as reported by Guiot and Spalla (2013). Briefly, 34.1 mg of TiO₂ nanopowders were added to 10 ml of HNO₃ 10⁻² M, then the suspension was sonicated for 20 min at 40% amplitude (sonicator: Bandelin Sonopuls HD2070, Germany). To 7.5 ml of the sonicated suspension were added 2.5 ml of sterile-filtered solution of BSA (10.24 mg/ml), then the pH was adjusted to 7 with NaOH 10⁻¹ M and NaOH 10⁻² M. Subsequently, this stock suspension was used to make appropriate dilutions in culture medium for the cell treatments. Cells in culture media supplemented with vehicle

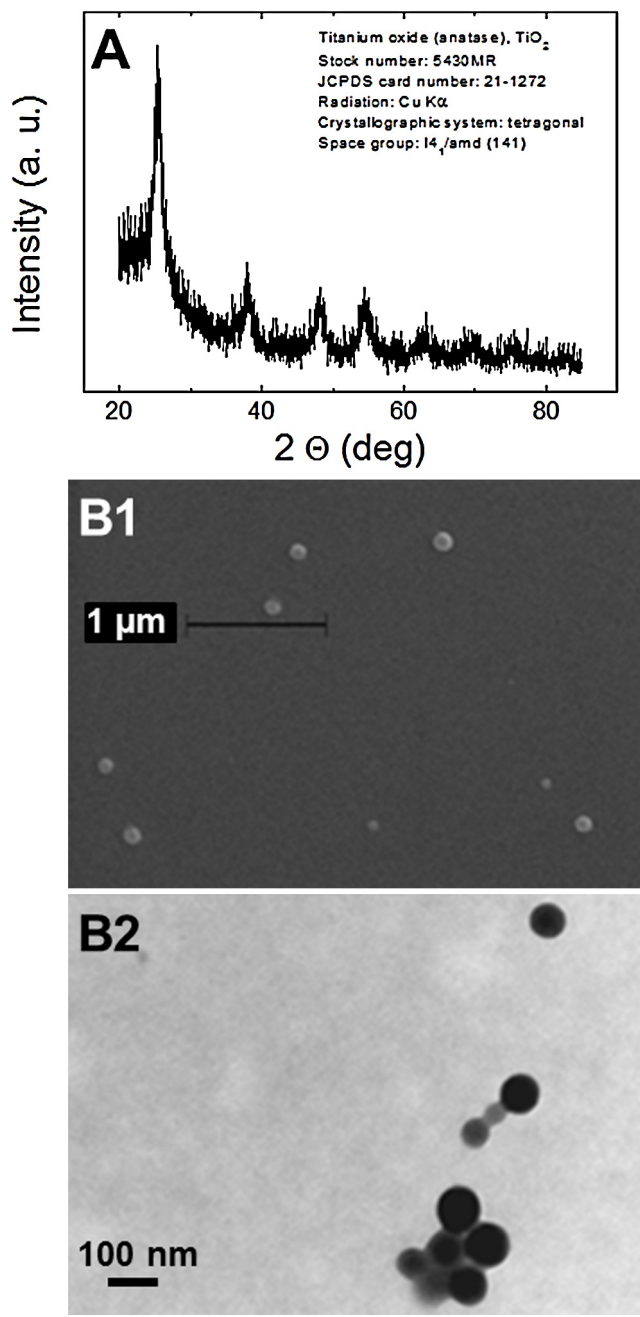


Fig. 1. Titanium dioxide nanoparticles confirmed by X-ray diffraction analysis (A, data provided by the Company). Morpho-dimensional analysis of the raw nanomaterial by TEM (B1) and SEM (B2). DLS indicated a diameter size of 69.3 ± 0.4 nm.

solution (HNO_3 10⁻² M plus BSA (10.24 mg/ml)) 2.5% (for doses ranging from 1.5 to 31 $\mu\text{g}/\text{ml}$) or 9.8% (for doses ranging from 62 to 250 $\mu\text{g}/\text{ml}$) acted as controls. The same procedure protocol was also used to make TiO_2 bulk suspension. Fresh suspensions of test materials were prepared shortly before each experiment. The stock suspension of both TiO_2 NP and TiO_2 bulk appears as a white colloidal dispersion.

2.4.1. Phase-contrast microscopy

To monitor the TiO_2 suspension solutions, applied into cell culture medium, the cells, were observed in phase-contrast microscopy after TiO_2 NP or TiO_2 bulk treatments (1.5, 15, 31, 62, 125, 250 $\mu\text{g}/\text{ml}$), and different time of exposure (from 4 to

48 h) in order, to obtain a better understanding of the effects on cell adherence, cell morphology and culture growth and to observe presence or absence of TiO_2 NP sediments. The cells, in the wells, were examined under Zeiss Axiovert 25 microscope using phase contrast objectives (32 \times magnification) and combined with a digital camera (Canon powershot G8). Digital photographs were taken from each well and stored on the PC.

2.5. Acute exposure (4–48 h)

2.5.1. Mitochondrial function (MTT assay)

The MTT assay was used to evaluate mitochondrial metabolism. Cells were seeded in 96-well plates (1×10^4 cells/well in 100 μl complete medium/well) 24 h before treatment. Experimental setup details consisted: 360 μl total volume of each well, 0.32 cm^2 the growth area, 100 μl the working volume/well, 10 μl the treatment volume/well.

Cells were exposed to TiO_2 NP and TiO_2 bulk at nominal mass concentrations ranging from 1.5 to 250 $\mu\text{g}/\text{ml}$ for 4, 24 and 48 h at 37 °C. After incubation, the cell culture media were carefully aspirated, the cells were washed with PBS (100 $\mu\text{l}/\text{well}$) to avoid the interference with the spectrophotometric analysis, then fresh medium plus 10 μl of MTT (5 mg/ml) was added to each well and incubated for 3 h. The resulting formazan crystals were solubilized by DMSO 100 $\mu\text{l}/\text{well}$ and quantified by measuring absorbance at 550 nm by BioRad microplate reader. Data were expressed as a percentage of control.

2.5.2. Membrane integrity (calcein AM/PI staining)

The membrane integrity and cell morphology were evaluated after TiO_2 NP and TiO_2 bulk (from 1.5 to 250 $\mu\text{g}/\text{ml}$, for 4, 24, 48 h) by cell co-incubation of 2 μM calcein-AM and 2.5 $\mu\text{g}/\text{ml}$ PI for 10 min at 37 °C. Test was performed in 96-well plates, the experimental setup details were: 360 μl total volume of each well, 0.32 cm^2 the growth area, 100 μl the working volume/well, 10 μl the treatment volume/well.

Cells were examined under a Zeiss Axiovert 25 fluorescence microscope provided with a triple filter set (excitation: 400, 495, 570 nm; beam splitter: 410, 505, 585 nm; emission: 460, 530, 610 nm), and combined with digital camera (Canon powershot G8). The images were captured using 32 \times objective lens and stored on a PC. Viability was evaluated and expressed as percentage cells retained calcein (green fluorescence) compared to the total cells counted (calcein-positive plus PI-positive (red fluorescence)), six fields/well were analyzed.

2.6. Prolonged exposure (7–10 days)

2.6.1. Growth and cell proliferation

The procedure for clonogenic assay applied to CNS cells was previously described (De Simone et al., 2013b). Briefly, cells were seeded in six-well plates at density of 300 cells/well for SH-SY5Y cells and 50 cells/well for D384 cells. Experimental setup details were: 16.8 ml of total volume/well, 9.5 cm^2 of growth area/well, 2 ml of working volume/well, 200 μl treatment volume/well. After attachment (about 20 h for SH-SY5Y and 4 h for D384 cells) the cells were washed with 2 ml PBS and treated with TiO_2 NP or TiO_2 bulk (final nominal mass concentration ranging from 0.05 to 31 $\mu\text{g}/\text{ml}$), over a time period required to form colonies (about 10 days for SH-SY5Y and 7 days for D384 cells). At the end of the treatment, the medium was removed and the colonies were washed, fixed, stained with hematoxylin, and let dry. Then, the colonies were manually counted for the evaluation of cell survival after TiO_2 NP treatments. The minimum size of colony was considered to be 50 cells/colony. The colonies were examined under Zeiss Axiovert 25 microscope combined with a

digital camera (Canon powershot G8). Digital photographs were taken from each well using $2.5\times$ objective lens. The number of colonies that arose after treatment was expressed in terms of plating efficiency (PE). PE was calculated by dividing the number of colonies formed by the number of cells plated per 100:

$$PE = \frac{\text{No. of colonies formed}}{\text{No. of cells seeded}} \times 100$$

2.7. Statistical analysis

Data from acute exposure were obtained from three independent experiments, each experiment was carried out in six replicates. Data from prolonged exposure were obtained from two independent experiments and each experiment was carried out in three replicates. Results are expressed as mean \pm S.D. Statistical analysis was performed by one-way ANOVA followed by Tukey's test (for each time point). A value of $P < 0.05$ was considered statistically significant.

3. Results

3.1. Characterization of TiO_2 NP in stock suspension and cell culture media

In the stock suspension, the dynamic light scattering (DLS) observation showed that a wide range of particle size distribution in the stock solution after 24 h from 10 to 1000 nm due to the aggregation or agglomeration. The mean hydrodynamic diameter was 52 nm, with a polydispersity index (PDI) of 0.444. These values were evaluated as volume% and intensity%, the latter presented in graph form (Fig. 2). The positive zeta potential (ZP) (0.35 mV) was indicative of a weak surface positive charge and the low value revealed a poor stability over time (a ZP of at least 30 mV (positive or negative) is required to achieve a reasonably stable dispersion).

When TiO_2 NPs were dispersed in culture media the size distribution of the TiO_2 NPs after 24 h was similar in DMEM and Ham's F12 media showing a mean hydrodynamic diameter of 356 and 299 nm, and PDI of 0.289 and 0.346, respectively. Again, the low zeta potentials (0.95 and 2.58 mV, respectively) were indicative of a poor stability over time.

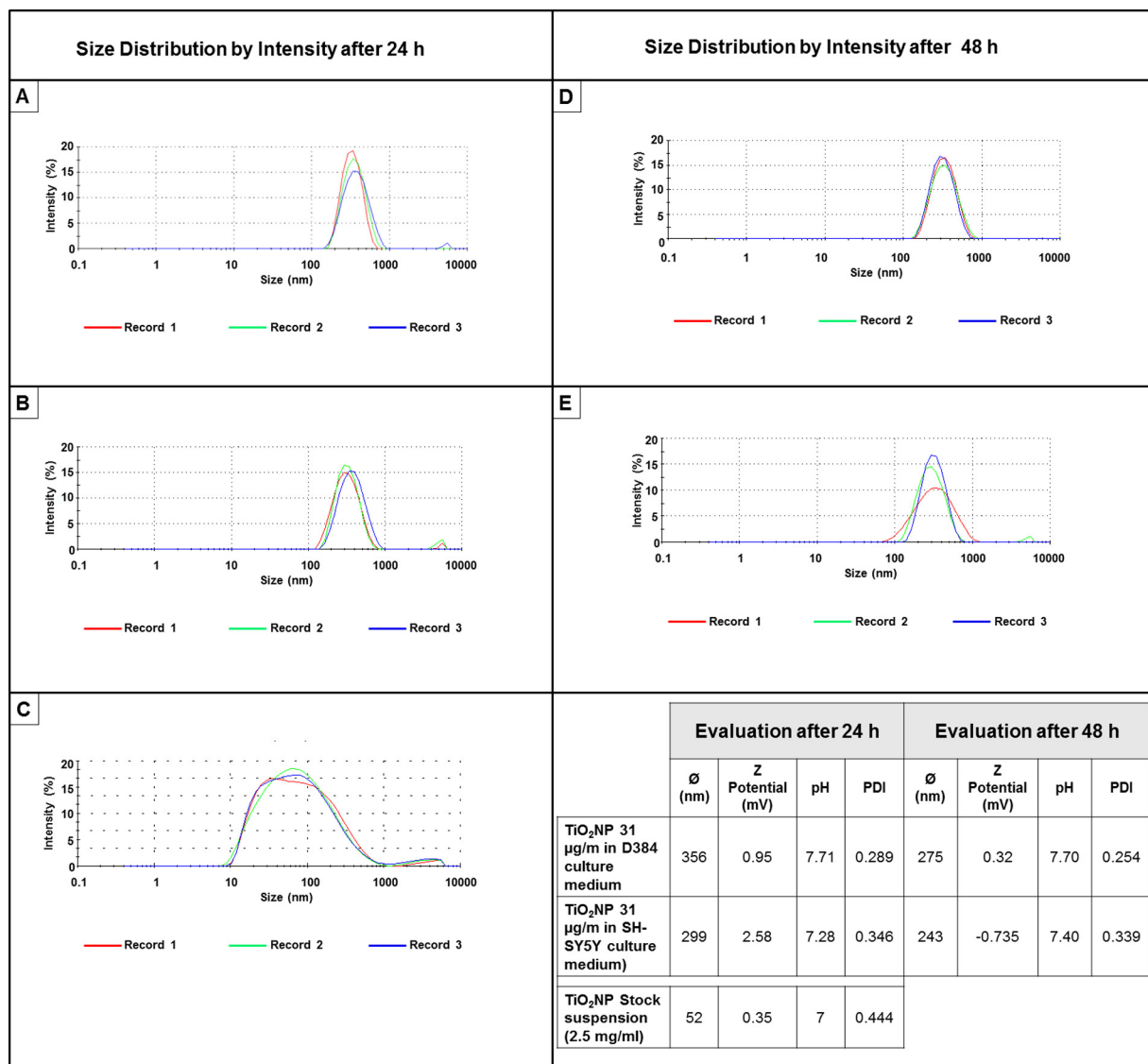


Fig. 2. Size distribution obtained from DLS measurements of TiO_2 NPs in D384 (A and D) and SH-SY5Y (B and E) culture media at the dose of 31 μ g/ml after 24 and 48 h. Size distribution of TiO_2 NP stock solution (2.5 mg/ml) is shown in panel (C). TiO_2 NP values of size distribution, z potential and polydispersity index (PDI) are reported in the table.

After 48 h, the size distribution of the TiO₂NPs were still similar in two culture media (mean hydrodynamic diameter of 275 and 243 nm, and PDI of 0.254 and 0.339, for DMEM and Ham's F12 respectively), accompanied with conspicuous white sediments observable to the naked eye in all samples. The ZPs (0.32 and -0.735 mV, respectively) were still low. In addition, TiO₂NP stock suspension had pH 7 and this value was close to the Point of Zero Charge (PZC) of TiO₂NPs and a faint increase of pH could change the sign of the ZP value (see table in Fig. 2). As a matter of fact, in the DMEM medium the pH is about stable (7.7) and the variation in time of the ZP value is not significant. In the Ham's F12 medium there is a slight increase of the pH (from 7.28 to 7.40) in time and this can justify an appreciable variation of ZP (about 3.5 points).

3.2. Cytotoxic effects – acute exposure (4–48 h)

3.2.1. Mitochondrial activity

Data regarding the mitochondrial function activity obtained by MTT assay are shown in Fig. 3. The trend of the mitochondrial activity was expressed as a percentage of cell viability relative to the vehicle, in particular 2.5% vehicle indicated as control for the lower doses tested of TiO₂NPs or TiO₂ bulk (1.5, 15, 31 μ g/ml) and 9.8% vehicle as control for the higher doses of TiO₂NP or TiO₂ bulk (62, 125, 250 μ g/ml).

At 4-h time point, both TiO₂NP and TiO₂ bulk treatments did not show any significant cytotoxic effect for all the tested doses (1.5–250 μ g/ml) on both cerebral cell lines (Fig. 3A and a), while the mitochondrial activity was affected by both compounds after 24 and 48 h exposure on both cerebral cells with a more pronounced effects of TiO₂NP compared to the bulk counterpart.

In particular, in D384 cells after 24 h, TiO₂NPs induced a mitochondrial damage starting at 31 μ g/ml with about 25% cell viability decrease, while TiO₂ bulk showed its effect starting at the dose of 125 μ g/ml with a reduction of about 20% (Fig. 3B).

TiO₂NP treatments on SH-SY5Y started to significantly affect mitochondrial metabolism at the dose of 15 μ g/ml (22% cell death), and TiO₂ bulk at 62 μ g/ml causing 17% cell decrease (Fig. 3b).

After 48 h, D384 cells showed a decrease of cell viability (20–55%) at TiO₂NP doses ranging from 31 to 250 μ g/ml and 20–38% reduction at TiO₂ bulk doses from 125 to 250 μ g/ml (Fig. 3C). SH-SY5Y cells displayed about 30–60% cell death at TiO₂NP doses ranging from 15 to 250 μ g/ml and 20–32% at TiO₂ bulk doses ranging from 62 to 250 μ g/ml (Fig. 3c).

Data comparison indicated that the TiO₂ bulk caused less effects on mitochondrial metabolism compared to those induced by the nanoparticle form. Notably higher susceptibility was observed for the SH-SY5Y compared to D384 for both materials (TiO₂NPs and TiO₂ bulk) after 24 and 48 h exposure.

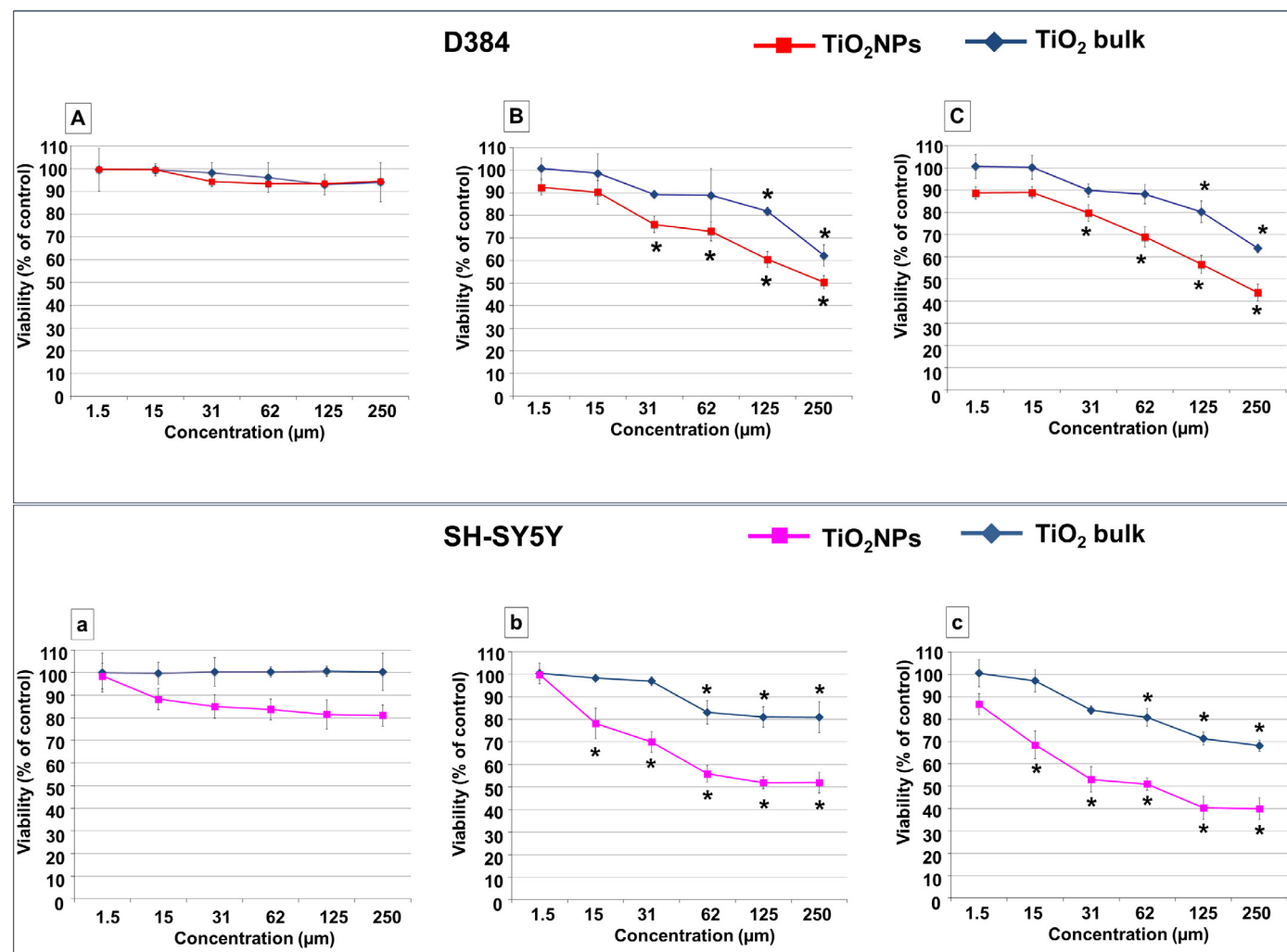


Fig. 3. Mitochondrial function evaluation by MTT assay in D384 and SH-SY5Y cells exposed to increasing concentrations (1.5–250 μ g/ml) of TiO₂NPs and TiO₂ bulk after 4 h (A and a), 24 h (B and b), and 48 h (C and c). Data are expressed mean \pm S.D. *Different from control in each cell line $P < 0.05$, statistical analysis by ANOVA followed by Tukey's test.

3.2.2. Cell membrane integrity and morphology

Membrane integrity and cell morphology were evaluated by calcein-AM/PI staining after 4, 24, and 48 h exposure to increasing concentrations of TiO_2 NPs or TiO_2 bulk (1.5–250 $\mu\text{g}/\text{ml}$).

The cellular membranes and morphology of D384 cells were not affected by TiO_2 NP or TiO_2 bulk treatments at the doses $\leq 62 \mu\text{g}/\text{ml}$ for each considered time point (4, 24 and 48 h) as evidenced by the green fluorescence uniformly diffused into cellular cytoplasm (data not shown). Instead, the membrane integrity of D384 cells

was affected (as evidenced by the presence of red colored cells) at the higher doses of 125 and 250 $\mu\text{g}/\text{ml}$ of both compounds after both 24 and 48 h exposure with TiO_2 bulk causing a less pronounced effect than that caused by nanoparticles (Fig. 4A). The cell morphology was also altered compared to the control at the higher doses (125 and 250 $\mu\text{g}/\text{ml}$) of both materials tested after both time points (24–48 h), in particular the treated cells lost the typical star-shaped morphology of cells arranged in a monolayer and likely formed islands/agglomerations (Fig. 4A).

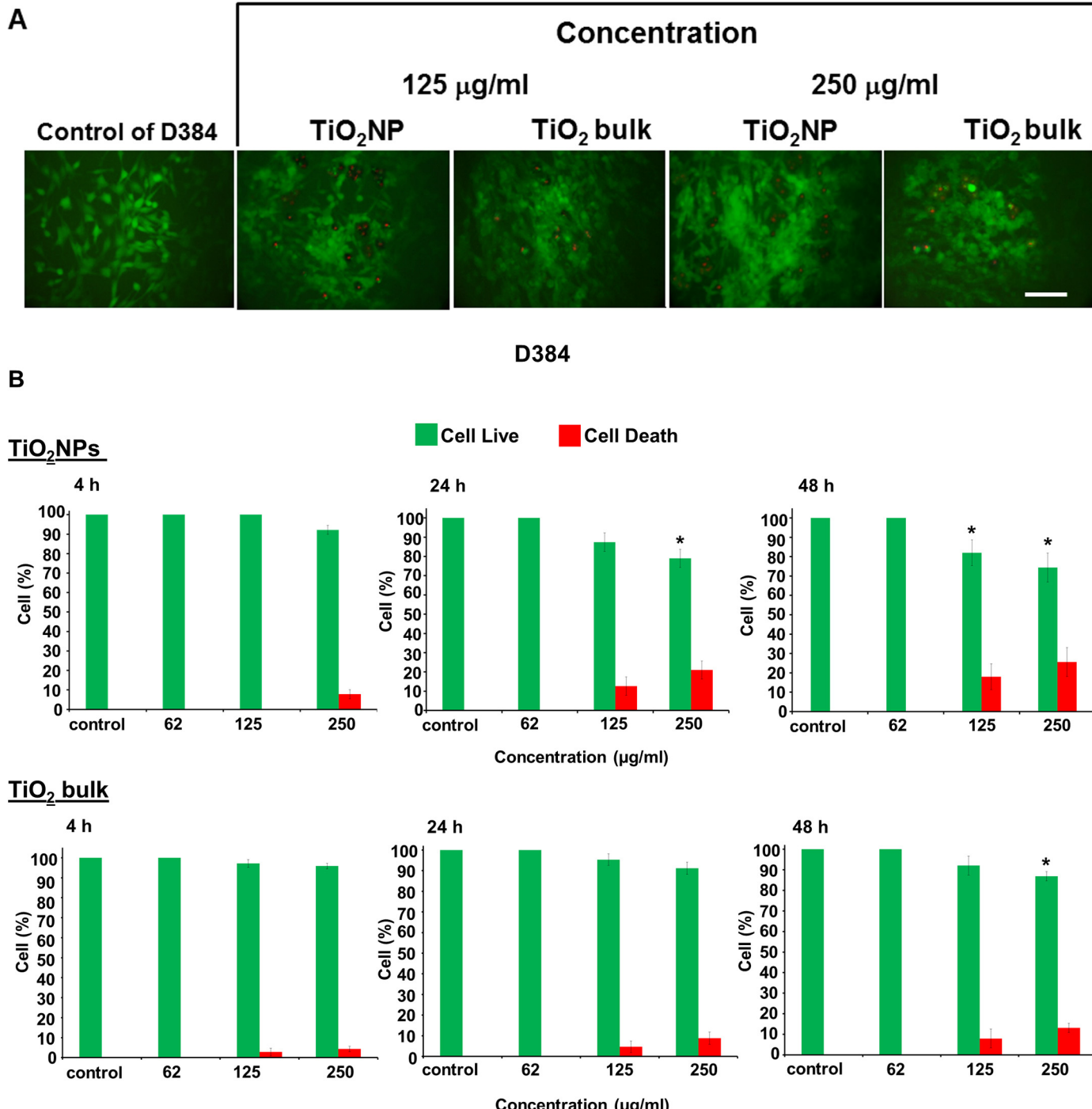


Fig. 4. Membrane integrity and cell morphology evaluation by calcein-AM/PI (A): representative images of randomly selected microscopic fields of D384 cells treated with the higher concentrations of TiO_2 NPs or TiO_2 bulk (125–250 $\mu\text{g}/\text{ml}$) after 48 h. The loss of membrane integrity was evidenced by red cell fluorescence. The cell morphology was also altered compared to the control: the cells lost the typical star-shaped cell and the arrangement in the monolayer. The effects induced by TiO_2 NPs were more pronounced than TiO_2 bulk (scale bar: 100 μm). Quantitative analysis (B) of the cell loss at the higher doses of TiO_2 NPs or TiO_2 bulk (62–250 $\mu\text{g}/\text{ml}$) after 4, 24 and 48 h. Data are the mean \pm S.D.

A similar pattern to D384 cells was also observed for neuroblastoma cells after TiO_2NP or TiO_2 bulk treatment. Indeed, SH-SY5Y membrane integrity (presence of red colored cells) and morphology, as evidenced by the lost the typical pyramidal-shaped and the tendency to form islands/agglomerations, were affected at the higher doses of 125 and 250 $\mu\text{g}/\text{ml}$ of both compounds tested after both 24 and 48 h (Fig. 5A).

Semi-quantitative analysis on D384 and SH-SY5Y cells was used to quantify the cell live and cell death after 4, 24 and 48 h exposure to increasing concentrations of TiO_2NPs or TiO_2 bulk (1.5–250 $\mu\text{g}/\text{ml}$; Figs. 4B and 5B show 62–250 $\mu\text{g}/\text{ml}$).

Glial cell viability data indicated that both types of treatments (TiO_2NP and TiO_2 bulk) did not affect the cell viability with the exception of the higher doses tested (125–250 $\mu\text{g}/\text{ml}$): cellular decrease of about 18–26% for TiO_2NP after 24 and 48 h. TiO_2 bulk caused 13% decrease viability only after 48 h at 250 $\mu\text{g}/\text{ml}$ (Fig. 4B).

A similar pattern of cell viability was also observed for SH-SY5Y cells at $\geq 125 \mu\text{g}/\text{ml}$: about 13–20% cell death after 24 and 48 h to TiO_2NP exposure; TiO_2 bulk caused about 13% decrease viability only after 48 h (Fig. 5B).

Figs. 6 and 7 showed a panel of representative randomly selected microscopic fields by phase-contrast microscopy for D384

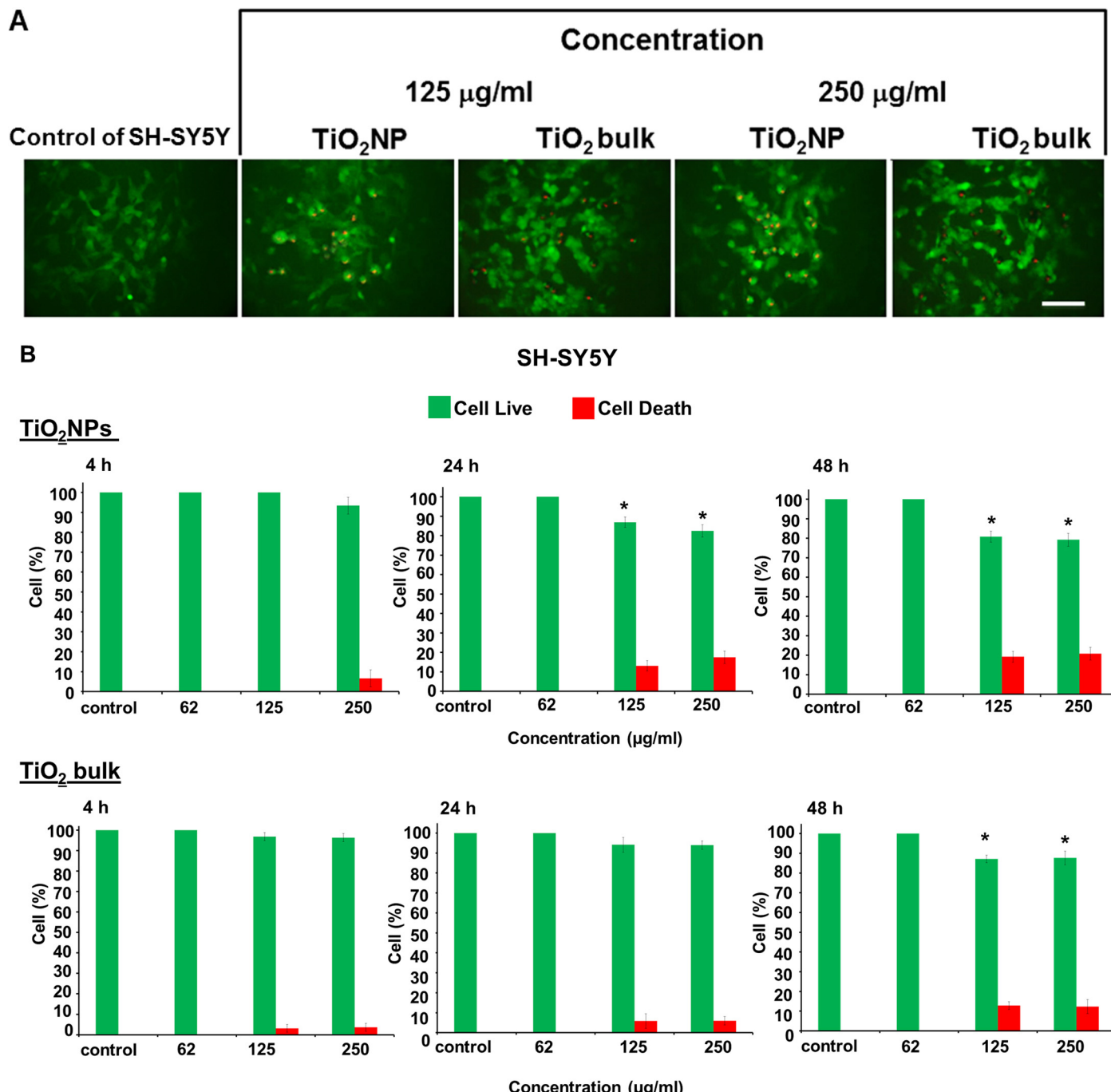
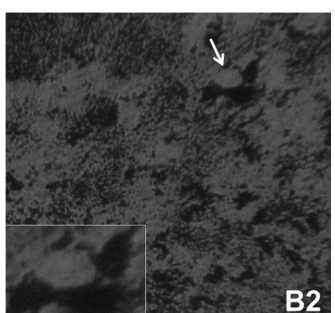
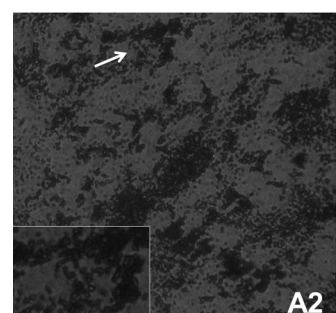
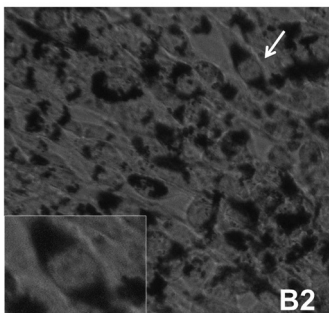
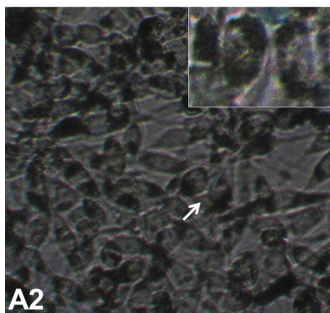
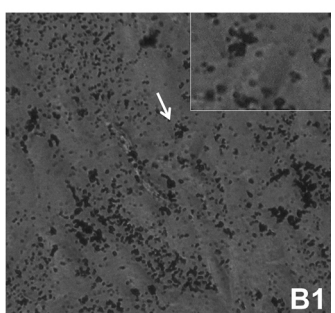
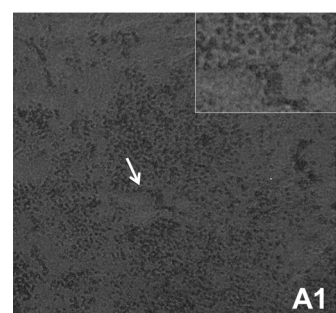
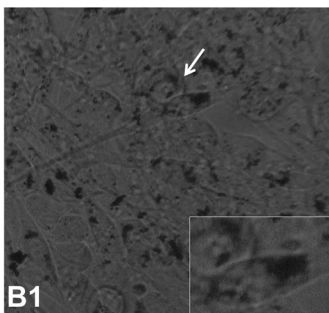
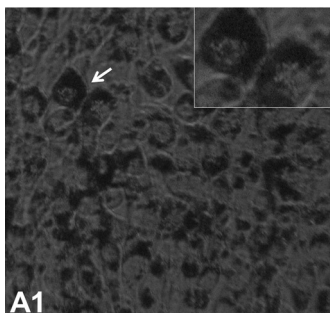
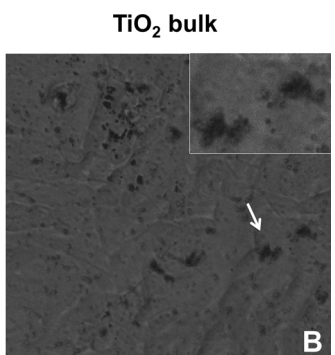
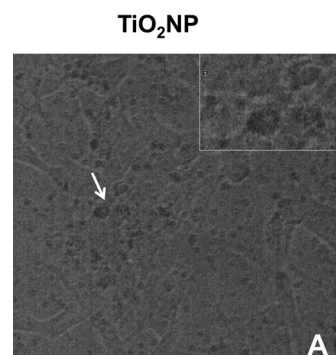
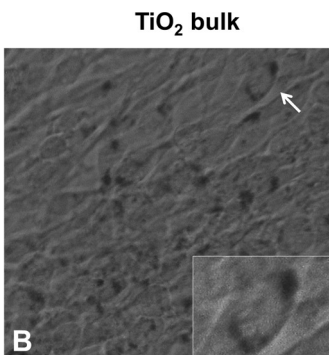
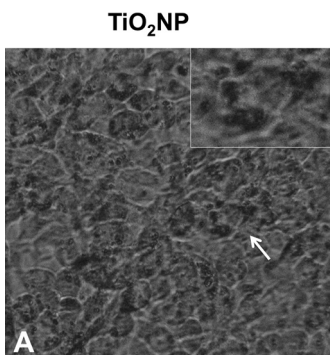
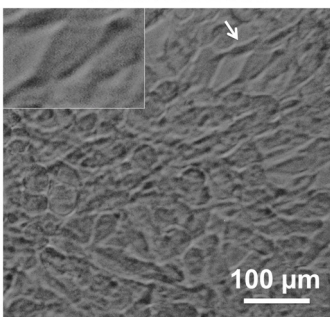


Fig. 5. Membrane integrity and cell morphology evaluation by calcein-AM/PI (A): representative images of randomly selected microscopic fields of SH-SY5Y cells treated with the higher concentrations of TiO_2NPs or TiO_2 bulk (125–250 $\mu\text{g}/\text{ml}$) after 48 h. The membrane damage was evidenced by red colored cells, in addition the pyramidal-shaped cell and the arrangement in the monolayer cells were lost, the effect rank: $\text{TiO}_2\text{NPs} > \text{TiO}_2\text{bulk}$ (Scale bar: 100 μm). Quantitative analysis (B) at the higher concentrations of TiO_2NPs or TiO_2 bulk (62–250 $\mu\text{g}/\text{ml}$) after 4, 24 and 48 h. Data are the mean \pm SD.



Control of D384



Control of SH-SY5Y

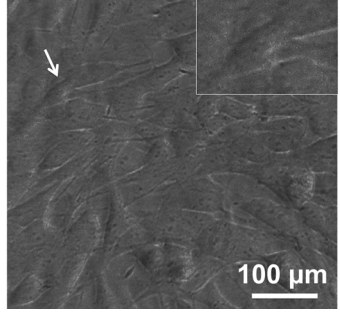


Fig. 6. Cellular morphology of astrocytoma D384 cells: representative images of randomly selected phase-contrast microscopic fields of D384 cells treated with concentrations: 15 µg/ml (A and B), 31 µg/ml (A1 and B1) and 125 µg/ml (A2 and B2) of TiO₂NPs or TiO₂ bulk after 48 h. The D384 cell images indicated alterations of cellular form (roundish-shaped instead of star-shaped cells) at the dose of 125 µg/ml after exposure to TiO₂NP or TiO₂ bulk only. Brownish sediments of both materials in the culture medium was observed at doses \geq 15 µg/ml. Inserts show the magnifications (2 \times) of the areas indicated by the arrows where TiO₂NPs and TiO₂ bulk are visible inside of the D384 cells (Scale bar: 100 µm).

and SH-SY5Y cells respectively, treated with increasing concentrations of TiO₂NPs or TiO₂ bulk (15, 31 and 125 µg/ml after 48 h), in order, to obtain a better understanding of the effects on cell adherence, cell morphology and culture growth of living cells and to observe presence or absence of sediments.

The evaluation of the images indicated no alterations of cellular form and structure in both cell lines (D384: Fig. 6A, B, B1 and

Fig. 7. Cellular morphology of neuroblastoma SH-SY5Y cells: representative images of randomly selected phase-contrast microscopic fields of D384 cells treated with concentrations: 15 µg/ml (A and B), 31 µg/ml (A1 and B1) and 125 µg/ml (A2 and B2) of TiO₂NPs or TiO₂ bulk after 48 h. Brownish sediments of both materials in the culture medium was observed at doses \geq 15 µg/ml, while at the dose of 125 µg/ml they totally masked the microscopy cell visualization of SH-SY5Y cells. Inserts show the magnifications (2 \times) of the areas indicated by the arrows (Scale bar: 100 µm).

SH-SY5Y: Fig. 7A, A1, B, B1) after exposure to TiO₂NP or TiO₂ bulk concentrations up to 31 µg/ml after 48 h.

Even though a specific protocol was applied to prepare finely dispersed suspensions, TiO₂NP and TiO₂ bulk brownish sediments of particles (detected by phase-contrast microscopy) in the culture medium were observed at doses \geq 15 µg/ml already after 4 h in both cell lines. This behavior is expected because the Point of Zero Charge (PZC) of these NPs, which represents the point of maximum instability of the dispersion (i.e. at ZP = 0 the NPs coalesce), is

around pH 7, that is the typical pH necessary to lead biomedical tests. This instability is verified by means of ZP measurements that reveal values very close to zero.

At doses of $\geq 62 \mu\text{g/ml}$ these sediments covered cell surface totally masking the light microscopy cell visualization of SH-SY5Y cells (Fig. 7A2), while cell morphology alteration could be appreciated for D384 (*i.e.*, roundish-shaped instead of star-shaped cells: Fig. 6A2) since a mild sedimentation was observable. Similar phenomenon was observable for TiO_2 bulk (Figs. 7B2 and 6B2).

Notably, a dose- and time-dependent accumulation of visible brown bodies were also evidenced inside of the D384 cells after TiO_2 NP and TiO_2 bulk treatments (Fig. 6 inserts).

3.3. Cytotoxic effects – prolonged exposure (7–10 days)

3.3.1. Growth and cell proliferation

To determine whether the prolonged exposure (up to 10 days) to increasing low concentrations (0.05–31 $\mu\text{g/ml}$) of TiO_2 NPs and TiO_2 bulk might cause effects, the proliferation ability (*i.e.* colony size) and colony forming capacity (*i.e.* cell growth and colony number) of brain cells were evaluated. The 2.5% vehicle was used as control. Figs. 8 and 9 show representative images of randomly selected light microscopic fields of the D384 and SH-SY5Y cells, respectively, after TiO_2 NP and TiO_2 bulk treatments. The colonies of vehicle were not different respect to untreated cells.

The images of D384 and SH-SY5Y colonies showed that the colony size decreased in a dose-dependent fashion starting at the dose of 1.5 $\mu\text{g/ml}$ for D384 (Fig. 8) and 0.1 $\mu\text{g/ml}$ for the SH-SY5Y (Fig. 9) after TiO_2 NPs but not after TiO_2 bulk.

Colony morphology alteration was observed after both materials tested starting at 0.2 $\mu\text{g/ml}$ for both cell lines (Figs. 8 and 9).

Sediments were observed at the highest doses (15 and 31 $\mu\text{g/ml}$) for both TiO_2 NP and TiO_2 bulk in both cell lines. Remarkably, visible brown bodies inside of both cell types, although less for SH-SY5Y, were observed after TiO_2 NP and TiO_2 bulk at the higher doses tested (15–31 $\mu\text{g/ml}$; Figs. 8 and 9 inserts).

Semi-quantitative analysis of D384 cells showed a dose-dependent reduction of the colony number of about 15–40% at TiO_2 NPs doses ranging from 0.2 to 31 $\mu\text{g/ml}$, while TiO_2 bulk did not affect the colony number (Fig. 10). SH-SY5Y cells displayed a similar pattern of colony decrease: 12–46% at TiO_2 NPs doses ranging from 0.2 to 31 $\mu\text{g/ml}$ and no effects of TiO_2 bulk on this parameter was still observed (Fig. 11).

4. Discussion

This study asked if TiO_2 NPs were neurotoxic to human astrocytes and neurons *in vitro* by a multiparametric method approach which included the evaluation of different endpoints *via* multiple assays and if that toxicological profile was (dis)similar to that caused by the bulk form.

Apart from the NIOSH (2011) recommended REL, to date, no occupational or environmental exposure limits for TiO_2 NPs have been set by any other regulatory agency, although various studies on modeling and analytical methodologies have been published in order to predict the environmental concentration of nanoparticles (Gottschalk et al., 2013). Consumer and environmental exposure levels are still unknown, and since these levels would be needed to test at “real world risk” levels, the cell-based cytotoxic assays, using representative CNS cell lines, were conducted not only at overexposure condition but even at acutely sub-lethal doses, as well as after prolonged exposure (up to 10 days) to non-cytotoxic concentrations (0.05–1.5 $\mu\text{g/ml}$).

The major results obtained after acute exposure showed that TiO_2 NP treatment produced:

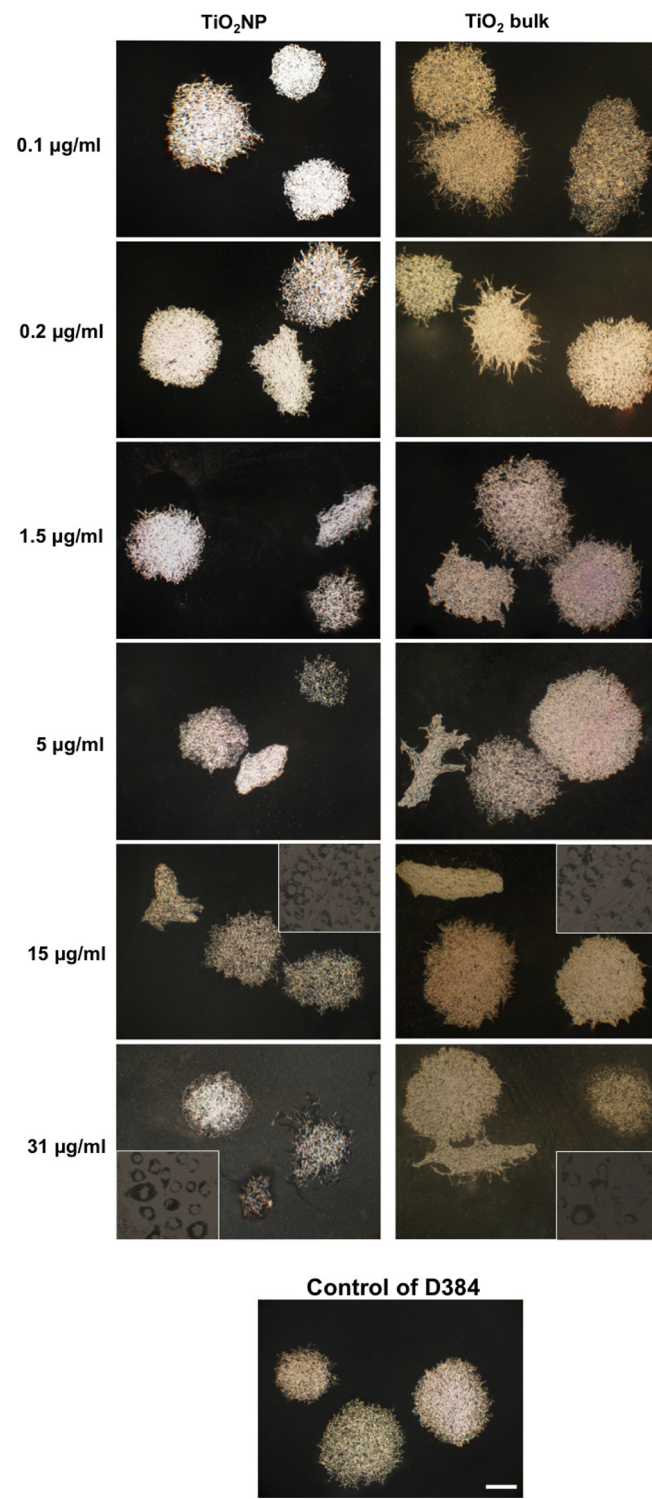


Fig. 8. Representative images of randomly selected microscopic fields of the colonies formed after 7 consecutive days exposure to increasing concentrations (0.1–31 $\mu\text{g/ml}$) of TiO_2 NPs or TiO_2 bulk. D384 colonies treated with TiO_2 NPs showed a reduction on size starting at the dose of 1.5 $\mu\text{g/ml}$, and the alterations of colony morphology starting at the dose of 0.2 $\mu\text{g/ml}$, while the TiO_2 bulk treatments induced morphology alteration only (Scale bar: 600 μm). *Inset:* Detail of a colony in phase-contrast microscopy (before staining), brownish bodies are visible inside D384 cells at the higher doses tested (15–31 $\mu\text{g/ml}$). (For interpretation of the references to color in this figure legend, the reader is referred to the web version of the article.)

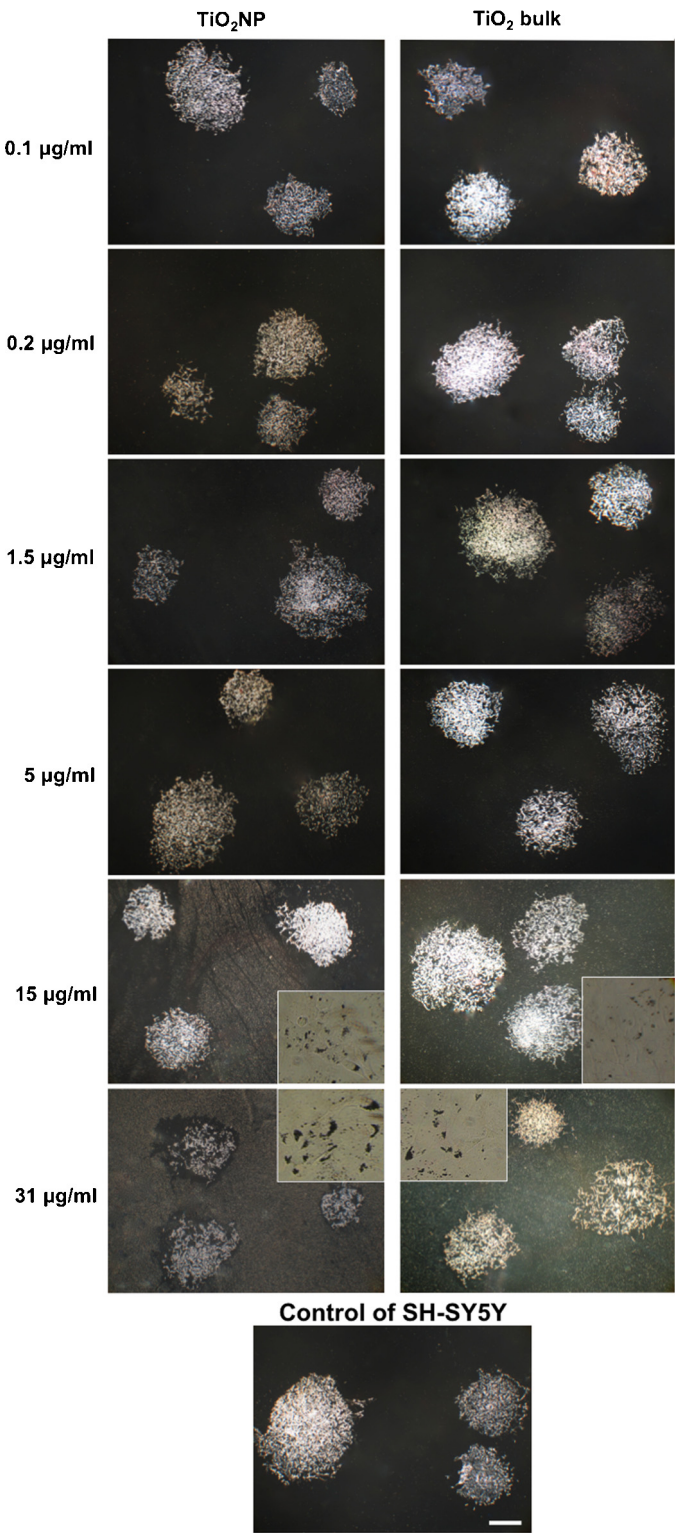


Fig. 9. Representative images of randomly selected microscopic fields of the colonies formed after 10 consecutive days of exposure to increasing concentrations (0.1–31 µg/ml) of TiO₂NPs or TiO₂ bulk. The colonies of SH-SY5Y treated with TiO₂NPs showed reductions on size and changes in colony morphology compared to control starting at the lowest dose of 0.1 µg/ml and 0.2 µg/ml, respectively, while the TiO₂ bulk treatment induced morphology alteration only (Scale bar: 600 µm). *Insert:* Detail of a colony in phase-contrast microscopy (before staining), brownish bodies are visible inside SH-SY5Y cells at the higher doses tested (15–31 µg/ml). (For interpretation of the references to color in this figure legend, the reader is referred to the web version of the article.)

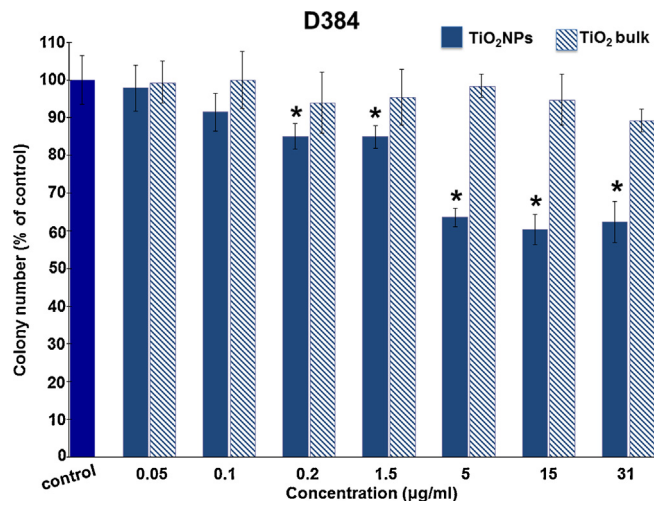


Fig. 10. Histograms display the number of colonies formed after 7 consecutive days of exposure to increasing concentration (0.05–31 µg/ml) of TiO₂NPs or TiO₂ bulk. No effect was observed on growth and cell proliferation after TiO₂ bulk treatment. Decrease in D384 colony number was 15–40% at the ranging dose from 0.2 to 31 µg/ml of TiO₂NPs. Data are expressed as percentage of respective control colonies. Error bars are \pm S.D. *Significant decrease of colony number: different from control ($P < 0.05$), statistical analysis by ANOVA followed by Tukey's test.

- (i) dose- and time-dependent alterations of the mitochondrial function on D384 and SH-SY5Y cells starting at the dose of 31 and 15 µg/ml, respectively, after 24 h exposure. SH-SY5Y were slightly more sensitive than D384 cells. The magnitude of effects on mitochondrial activity caused by TiO₂NPs was more pronounced compared to that produced by TiO₂ bulk whose effects appeared only at the highest doses (125 and 250 µg/ml) after 24 and 48 h, similarly in both cerebral cell lines;
- (ii) cell membrane damage starting at 125 µg/ml after 24 h exposure in both cerebral cells. The effects of TiO₂ bulk on membrane integrity were still less pronounced than those induced by nanoparticles.

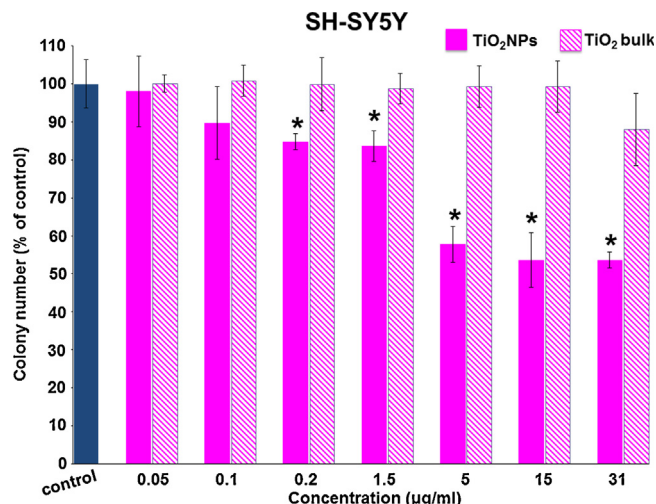


Fig. 11. The number of colonies formed after 10 consecutive day exposure to increasing concentrations of TiO₂NPs and TiO₂ bulk (0.05–31 µg/ml) are represented as histograms. The formation of SH-SY5Y colonies appeared to be compromised at the TiO₂NP dose of 0.2 µg/ml with a decrease 15% up to a maximum reduction of 46% at a dose of 31 µg/ml. No effects on growth and cell proliferation were observed after exposure to TiO₂ bulk. Error bars are \pm S.D. *Significant decrease of colony number: different from control ($P < 0.05$), statistical analysis by ANOVA followed by Tukey's test.

An apparent dose-dependent intracellular accumulation of TiO₂NP and TiO₂ bulk, although less evident for the latter, was observed in D384 cells by phase contrast light microscopy. TiO₂ (nanoparticulate and bulk form) internalization in SH-SY5Y other than D384 cells could be appreciated using the clonogenic test.

Data achieved after prolonged exposure (up to 10 days) revealed that the cell proliferative capacity, in term of colony size, were compromised at the extremely TiO₂NP low doses of 1.5 µg/ml and 0.1 µg/ml for D384 and SH-SY5Y, respectively, thus indicating the higher sensitivity of the SH-SY5Y compared to D384. On the other hand, the colony number decrease (15%) was evident at 0.2 µg/ml TiO₂NP dose for both cerebral cell types, indicating that the cell growth of both D384 and SH-SY5Y was similarly affected. TiO₂ bulk treatment affected cell morphology only.

This is the first study to demonstrate human cerebral cells (astrocytes and neurons) sensitivity to TiO₂NP not only after acute but even after prolonged low dose exposure.

Up to now, indeed, the cytotoxic effects of TiO₂NPs have been demonstrated in rodent neuronal and microglial cells after acute TiO₂NP doses (effects from 10 to 16 µg/ml by using similar endpoints as those presently applied – MTT test and live/dead staining) (Liu et al., 2010; XiaoBo et al., 2009), and in human neuronal, glial or astrocytes-like cells again after acute exposure only in which cell cycle alterations, morphological changes, apoptosis/necrosis, oxidative stress, mitochondrial depolarization, cytoskeletal proteins changes have been shown (Huerta-García et al., 2014; Lai et al., 2008; Márquez-Ramírez et al., 2012; Valdiglesias et al., 2013).

Notably, our data suggest that TiO₂NPs can elicit cytotoxic effects (i.e., alteration of cell growth (colony number) and proliferation (colony size)) in human CNS cells after prolonged exposure (up to 10 days) at doses ranging from 0.1 to 1.5 µg/ml. As such, TiO₂NP was potent inhibitor of cell proliferation.

Although the cells applied in our study are derived from human brain tumors, SH-SY5Y cells are widely used in toxicological and metabolic studies since they provide similar biochemical characteristics to those of human DAergic neurons (Xie et al., 2010). Similarly, the D384 cells are used to study the neurotoxicity, functional and metabolic alterations of xenobiotics (Björklund et al., 2008; Castoldi et al., 2000; Darè et al., 2001; Goldoni et al., 2003).

These *in vitro* critical doses may assume a relevant consideration if related to the existing *in vivo* animal data (although still few) on Ti levels detected in brain regions after intranasal (i.n.) administration of low repeated doses of TiO₂NP (500 µg/mice). High Ti accumulation (ranging from 0.13 to 0.3 µg/ml) was detected in hippocampus, and resulted in: irregular arrangement and loss of neurons, morphological changes and oxidative damage (Wang et al., 2008a,b). Again, brain levels of 0.05–0.15 µg/ml were detected after i.n. administration of 50–1000 µg/mouse for 90 days in association with oxidative stress, overproliferation of all glial cells, tissue necrosis, hippocampal cell apoptosis (Ze et al., 2014b).

Based on these observations, and considering the important matter addressing the issue of the *in vivo* relevance of some *in vitro* assays for evaluating the toxicity of NPs (Han et al., 2012; Sayes et al., 2007), the TiO₂NP *in vivo* data seem to be an essential criterion for accepting the utility of these *in vitro* assays for TiO₂NP toxicity evaluation.

Our studies also suggested that these TiO₂ nanoparticles are taken up and accumulated in D384 cells. This phenomenon increases over time (from 4 to 48 h) or with the dose (from 15 to 250 µg/ml) and could be responsible, at least in part, of the intracellular toxicity (i.e. mitochondrial damage). As such likely, a less evident intracellular accumulation of TiO₂ bulk was associated to a minor effect (≥ 125 µg/ml) compared to TiO₂NP.

Indeed, studies on TiO₂NPs uptake, using flow cytometry and TEM, indicated that nanoparticles (350 nm size as aggregates) were internalized in cytoplasm vesicles by human astrocytoma U373 cell line after 24 h (Márquez-Ramírez et al., 2012).

With SH-SY5Y cells, NP internalization phenomenon was difficult to appreciate by phase-contrast microscopy. NP aggregation and sedimentation were observed at doses ≥ 62 µg/ml covering cell surface and masking their visualization, however, TiO₂NP uptake was appreciated by clonogenic assays.

Indeed, a recent study has demonstrated, using flow cytometry, anatase TiO₂NPs (at the ranging doses from 80 to 150 µg/ml; approximately hydrodynamic diameter of 500 nm) uptake in SH-SY5Y that resulted concentration-dependent and associated with cell cycle alterations, and apoptosis (Valdiglesias et al., 2013).

In our DLS measurements, the size distribution of TiO₂NPs indicated a lower mean diameter in stock solution (aqueous state) compared to that determined when NPs were dissolved in cell culture media. The increases in the hydrodynamic sizes obtained in complete culture media compared to the sizes in water might be due to agglomerations as depicted by phase-contrast micrographs and by light microscopy in prolonged exposure experiments. Indeed, some studies have been suggested that particle concentration and the presence of proteins in culture medium are factors that influence the colloidal stability (sedimentation/agglomeration) of TiO₂NPs (Allouni et al., 2009; Long et al., 2006; Márquez-Ramírez et al., 2012; Valant et al., 2012; Valdiglesias et al., 2013; Vamanu et al., 2008b; Xia et al., 2006). This phenomenon seems to represent a realistic aspect of the TiO₂NPs that should be considered as an intrinsic property during the evaluation process.

The present results obtained after prolonged treatment with TiO₂NP suggest that continuous exposure to low TiO₂NP doses (0.2 µg/ml) severely affected proliferation of both CNS cell types (SH-SY5Y and D384). Studies using the clonogenic assay to evaluate cell survival after exposure to nanomaterials are very limited. However, it has been found that this assay was suitable for testing the toxicity of carbon nanotubes (Gellein et al., 2009; Herzog et al., 2007), cadmium silica coated NPs (De Simone et al., 2013a), and silver NPs (Coccini et al., 2014).

SH-SY5Y cells were apparently slightly more susceptible against TiO₂NP treatment when compared with D384 cells during acute exposure (24–48 h) for mitochondrial metabolism (toxic effect at 15 µg/ml for SH-SY5Y and 31 µg/ml for D384) as well as after several day exposure (up to 10 days) to low doses for the colony size reduction as indicator of cell proliferation decrease at 0.1 (for SH-SY5Y) vs. 1.5 µg/ml (for D384). The high vulnerability of neurons other than astrocytes observed after exposure to low TiO₂NP doses, as demonstrated here, might thus have fundamental consequences on the proper function of neural networks. Astrocytes communicate with neurons to enable synapse formation, synaptic transmission, and synaptic homeostasis. In addition, astrocytes have the ability to respond dynamically to challenges that threaten internal homeostasis, phenomenon known as plasticity that may permit astrocytes under severe stress to better support neurons and help explain the protracted nature of neurodegeneration (Leak, 2014). The finding of our study is of special interest due to, on one side, the recognized particular role of astrocytes in several neurodegenerative diseases, being more likely the cell type initially affected during pathogenesis (Maramakis and Rothstein, 2006). On the other hand, astrocytes have a variety of important functions such as supplying of metabolic nutrients to neurons and protecting the brain against oxidative stress and metal toxicity (Eroglu and Barres, 2010; Hirrlinger and Dringen, 2010; Parpura et al., 2012; Tiffany-Castiglioni et al., 2011). In addition, several studies have also reported that the rate of nanoparticle translocation into the brain can be significantly

increased under certain pathological conditions, such as infection, meningitis, and systemic inflammation (Sharma and Sharma, 2007; Sharma et al., 2010).

In this investigation, TiO_2 bulk produced a smaller effect than TiO_2 NP or even no effect. In accordance, TiO_2 NPs were generally more toxic than corresponding bulk forms as evidenced in several *in vitro* studies (Becker et al., 2014; Gurr et al., 2005; Rahman et al., 2002). A dose-dependent effect on the human immune system was observed in isolated human peripheral blood mononuclear cells (PBMC) after TiO_2 NPs as well as TiO_2 bulk albeit somewhat weaker than TiO_2 NPs at doses from 9.4 to 150 $\mu\text{g}/\text{ml}$ (Becker et al., 2014). Gurr et al. (2005) obtained similar results in human bronchial epithelial (BEAS 2B) cells where TiO_2 NPs (anatase; 10 and 20 nm) induced oxidative DNA damage, lipid peroxidation and micronucleus formation whereas TiO_2 bulk did not. Rahman et al. (2002) compared the toxicity of TiO_2 NPs (20 nm) with that of bulk TiO_2 (≥ 200 nm) in syrian hamster embryo (SHE) cells and found significant effects of TiO_2 NPs only after 10–72 h.

A recent *in vivo* study also reported a more severe toxicity in the mouse brain of the anatase TiO_2 NPs, injected at the abdominal cavity, than that caused by TiO_2 bulk, since NPs were probably able to migrate into the brain more readily and be more absorbed from the circulation, compared to TiO_2 bulk (Ma et al., 2010). The TiO_2 NP concentration in the brain was increased as increases in dosages used, and high-dosages were associated to oxidative stress and injury of the brain, and subsequently disturbance of the normal metabolism of neurochemicals. Comparatively, the contents of titanium in the mouse brain from the bulk TiO_2 group were significantly lower and less severe brain toxicity was observed.

5. Conclusions

As there is not yet a generally applicable paradigm for nanomaterial hazard identification, a case-by-case approach for the risk assessment of nanomaterials is still warranted (EU, 2012). In particular, since not standardized tests for the evaluation of safety properties of NPs are available, the toxicological characterization must be carried out with the criteria, methods and strategies chosen on individual basis in relation to the nature and properties of the material under consideration.

The initial screening for nanotoxicity is preferably performed *in vitro*, with prominent need to identify reliable models with a higher predictive power, mimicking the *in vivo* environment more closely (Joris et al., 2013; Nel, 2013).

Specifically to the TiO_2 NP toxicity evaluation on CNS, the *in vivo* data, so far available, provide basic evidence for accepting the utility of the presently applied *in vitro* battery of tests, although not from a mechanistic in nature point of view, but at least in term of critical doses capable to induce brain cell effects observed after prolonged exposure (*i.e.*, 0.1–0.2 $\mu\text{g}/\text{ml}$ by *in vitro* vs. 0.05–0.15 $\mu\text{g}/\text{ml}$ by *in vivo* (Ze et al., 2014b)). Thus even though no meaningful predictions can be made for an *in vivo* outcome based on an *in vitro* endpoint, conversely, this *in vitro* battery of tests apparently showed to be predictive tools as alternative methods to *in vivo* procedures in line with regulatory requirements, limiting the use of laboratory animals (Hartung, 2009; Hartung et al., 2013).

Conflict of interest

The authors declare that there are no conflicts of interest.

Transparency document

The Transparency document associated with this article can be found in the online version.

Acknowledgements

This work was supported by Grants from Italian Ministries of Health, Research and Education and CARIPLO Foundation (Rif. 2011–2096).

References

- Allouni ZE, Cimpana MR, Høl PJ, Skodvind T, Gjerdet NR. Agglomeration and sedimentation of TiO_2 nanoparticles in cell culture medium. *Colloids Surf B Biointerfaces* 2009;68:83–7.
- Baan R, Straif K, Groosse Y, Secretan B, El Ghissassi F, Cogliano V. WHO international Agency for research on cancer monograph working group. Cancerogenicity of carbon black, titanium dioxide, and talc. *Lancet Oncol* 2006;4:295–6.
- Balmforth AJ, Ball SG, Freshney RI, Graham DL, McNamee HB, Vaughan PF. D-1 dopaminergic and β -adrenergic stimulation of adenylyl cyclase in a clone derived from the human astrocytoma cell line G-CCM. *J Neurochem* 1986;47(3):715–9.
- Becker K, Schroecksnadel S, Geisler S, Carriere M, Gostner JM, Schennach H, et al. TiO_2 nanoparticles and bulk material stimulate human peripheral blood mononuclear cells. *Food Chem Toxicol* 2014;65:63–9.
- Bermudez E, Mangum JB, Wong BA, Asgharian B, Hext PM, Warheit DB, et al. Pulmonary responses of mice, rats, and hamsters to subchronic inhalation of ultrafine titanium dioxide particles. *Toxicol Sci* 2004;77:347–57.
- Björklund O, Shang M, Tonazzini I, Daré E, Fredholm BB. Adenosine A1 and A3 receptors protect astrocytes from hypoxic damage. *Eur J Pharmacol* 2008;596:6–13.
- Brun E, Carrière M, Mabondoz A. In vitro evidence of dysregulation of blood-brain barrier function after acute and repeated/long-term exposure to TiO_2 nanoparticles. *Biomaterials* 2012;33:886–96.
- Castoldi AF, Barni S, Turin I, Gandini C, Manzo L. Early acute necrosis, delayed apoptosis and cytoskeletal breakdown in cultured cerebellar granule neurons exposed to methylmercury. *J Neurosci Res* 2000;59(6):775–87.
- Coccini T, Manzo L, Bellotti V, De Simone U. Assessment of cellular responses after short- and long-term exposure to silver nanoparticles in human neuroblastoma (SH-SY5Y) and astrocytoma (D384) cells. *ScientificWorldJournal* 2014;2014:259765. <http://dx.doi.org/10.1155/2014/259765> eCollection 2014.
- Daré E, Li W, Zhivotovsky B, Yuan X, Ceccatelli S. Methylmercury and H2O2 provoke lysosomal damage in human astrocytoma D384 cells followed by apoptosis. *Free Radic Biol Med* 2001;30(12):1347–56.
- De Simone U, Manzo L, Profumo A, Coccini T. In vitro toxicity evaluation of engineered cadmium-coated silica nanoparticles on human pulmonary cells. *J Toxicol* 2013a;2013:931785. <http://dx.doi.org/10.1155/2013/931785>.
- De Simone U, Manzo L, Ferrari C, Bakeine J, Locatelli C, Coccini T. Short and long-term exposure of CNS cell lines to BPA-f a radiosensitizer for boron neutron capture therapy: safety dose evaluation by a battery of cytotoxicity tests. *Neurotoxicology* 2013b;35:84–90.
- Douglas KE, Dirk V, Timothy MS, Bruce JS. Titanium nanoparticles move to the marketplace. *Chem Innov* 2000;30:30–5.
- Eroglu C, Barres BA. Regulation of synaptic connectivity by glia. *Nature* 2010;468:223–31.
- EU (European Commission), Brussels, 3.10.2012, COM (2012) 572 final. Communication from the commission to the European Parliament, the Council and the European Economic and Social Committee. Second Regulatory Review on Nanomaterials.
- Gellein K, Hoel S, Evje L, Syversen T. The colony formation assay as an indicator of carbon nanotube toxicity examined in three cell lines. *Nanotoxicology* 2009;3:215–21.
- Goldoni M, Vettori MV, Alinovi R, Cagliari A, Ceccatelli S, Mutti A. Models of neurotoxicity: extrapolation of benchmark doses in vitro. *Risk Anal* 2003;23(3):505–14.
- Gottschalk F, Sun TY, Nowack B. Environmental concentrations of engineered nanomaterials: Review of modeling and analytical studies. *Environ Pollut* 2013;181:287–300.
- Grassian VH, O'Shaughnessy PT, Adamcakova-Dodd A, Pettibone JM, Thorne PS. Inhalation exposure study of titanium dioxide nanoparticles with a primary particle size of 2 to 5 nm. *Environ Health Perspect* 2007;115(3):397–402.
- Guioit C, Spalla O. Stabilization of TiO_2 nanoparticles in complex medium through a pH adjustment protocol. *Environ Sci Technol* 2013;47:1057–64.
- Gurr JR, Wang AS, Chen CH, Jan KY. Ultrafine titanium dioxide particles in the absence of photoactivation can induce oxidative damage to human bronchial epithelial cells. *Toxicology* 2005;213:66–73.
- Han X, Corson N, Wade-Mercer P, Gellein R, Jiang J, Sahu M, et al. Assessing the relevance of *in vitro* studies in nanotoxicology by examining correlations between *in vitro* and *in vivo* data. *Toxicology* 2012;297(1–3):1–9.
- Hartung T. Food for thought... on alternative methods for nanoparticle safety testing. *ALTEX* 2009;27(2/10).
- Hartung T, Luechtefeld T, Maertens A, Kleensang A. Integrated testing strategies for safety assessments. *ALTEX* 2013;30:3–18.
- Herzog E, Casey A, Lyng FM, Chambers G, Byrne HJ, Davoren M. A new approach to the toxicity testing of carbon-based nanomaterials – the clonogenic assay. *Toxicol Lett* 2007;174:49–60.
- Hirrlinger J, Dringen R. The cytosolic redox state of astrocytes: maintenance, regulation and functional implications for metabolite trafficking. *Brain Res Rev* 2010;63:177–88.
- Huerta-García E, Pérez-Arizt JA, GisselaMárquez-Ramírez S, Delgado-Buenrostro NL, Chirino YI, Iglesias GG, et al. Titanium dioxide nanoparticles induce strong

- oxidative stress and mitochondrial damage in glial cells. *Free Radic Biol Med* 2014; <http://dx.doi.org/10.1016/j.freeradbiomed.2014.04.026>.
- Hu R, Gong X, Duan Y, Li N, Che Y, Cui Y, et al. Neurotoxicological effects and the impairment of spatial recognition memory in mice caused by exposure to TiO_2 nanoparticles. *Biomaterials* 2010;31(31):8043–50.
- Jin CY, Zhu BS, Wang XF, Lu QH. Cytotoxicity of titanium dioxide nanoparticles in mouse fibroblast cells. *Chem Res Toxicol* 2008;21:1871–7.
- Joris F, Manshian BB, Peynshaert K, De Smedt SC, Braeckmans K, Soenen SJ. Assessing nanoparticle toxicity in cell-based assays: influence of cell culture parameters and optimized models for bridging the in vitro–in vivo gap. *Chem Soc Rev* 2013;42(21):8339–59. <http://dx.doi.org/10.1039/c3cs60145e>.
- Kaida T, Kobayashi K, Adachi M, Suzuki F. Optical characteristics of titanium oxide interference film and the film laminated with oxides and their applications for cosmetics. *J Cosmet Sci* 2004;55:219–20.
- Kobayashi N, Naya M, Endoh S, Maru J, Yamamoto K, Nakanishi J. Comparative pulmonary toxicity study of nano- TiO_2 particles of different sizes and agglomerations in rats: different short- and long-term post-instillation results. *Toxicology* 2009;264:110–8.
- Kreyling WG, Semmler M, Erbe F, Mayer P, Takenaka S, Schulz H, et al. Translocation of ultrafine insoluble iridium particles from lung epithelium to extrapulmonary organs is size dependent but very low. *J Toxicol Environ Health A* 2002;65(20):1513–30.
- Lai JC, Lai MB, Jandhyam S, Dukhande VV, Bhushan A, Daniels CK, et al. Exposure to titanium dioxide and other metallic oxide nanoparticles induces cytotoxicity on human neural cells and fibroblasts. *Int J Nanomed* 2008;3:533–45.
- Leak RK. Adaptation and sensitization to proteotoxic stress. *Dose Response* 2014;12:24–56.
- Li Y, Li J, Li W, Kang C, Huang Q, Li Q. Systematic influence induced by 3 nm titanium dioxide following intratracheal instillation of mice. *J Nanosci Nanotechnol* 2010;10:8544–9.
- Liu S, Xu L, Zhang T, Ren G, Yang Z. Oxidative stress and apoptosis induced by nanosized titanium dioxide in PC12 cells. *Toxicology* 2010;267(1–3):172–7.
- Long TC, Saleh N, Tilton RD, Lowry GV, Veronesi B. Titanium dioxide (P25) produces reactive oxygen species in immortalized brain microglia (BV2): implications for nanoparticle neurotoxicity. *Environ Sci Technol* 2006;40:4346–52.
- Long TC, Tajuba J, Sama P, Saleh N, Swartz C, Parker J, et al. Nanosize titanium dioxide stimulates reactive oxygen species in brain microglia and damages neurons in vitro. *Environ Health Perspect* 2007;115:1631–7.
- Ma L, Liu J, Li N, Wang J, Duan Y, Yan J, et al. Oxidative stress in the brain of mice caused by translocated nanoparticulate TiO_2 delivered to the abdominal cavity. *Biomaterials* 2010;31(1):99–105.
- Ma-Hock L, Burkhardt S, Strauss V, Gamer AO, Wiench K, van Ravenzwaay B, et al. Development of a short-term inhalation test in the rat using nano-titanium dioxide as a model substance. *Inhal Toxicol* 2009;21:102–18.
- Maragakis NJ, Rothstein JD. Mechanisms of disease: astrocytes in neurodegenerative disease. *Nat Clin Pract Neurol* 2006;2:679–89.
- Márquez-Ramírez SG, Delgado-Buenrostro NL, Chirino YI, Iglesias GG, López-Marure R. Titanium dioxide nanoparticles inhibit proliferation and induce morphological changes and apoptosis in glial cells. *Toxicology* 2012;302(2–3):146–56.
- Montazer M, Seifollahzadeh S. Enhanced self-cleaning, antibacterial and UV protection properties of nano TiO_2 treated textile through enzymatic pretreatment. *Photochem Photobiol* 2011;87:877–83.
- Nel AE. Implementation of alternative test strategies for the safety assessment of engineered nanomaterials. *J Intern Med* 2013;274(6):561–77. <http://dx.doi.org/10.1111/joim.12109>.
- NIOSH. Occupational Exposure to Titanium Dioxide. In: Current Intelligence Bulletin 63. Cincinnati: National Institute for Occupational Safety and Health; 2011.
- Oberdörster G, Elder A, Rinderknecht A. Nanoparticles and the brain cause for concern? *J Nanosci Nanotechnol* 2009;9(8):4996–5007.
- Osiér M, Oberdörster G. Intratracheal inhalation vs. intratracheal instillation: differences in particle effects. *Fundam Appl Toxicol* 1997;40:220–7.
- Parpura V, Heneka MT, Montana V, Oliet SH, Schousboe A, Haydon PG, et al. Glial cells in (patho)physiology. *J Neurochem* 2012;121:4–27.
- Rahman Q, Lohani M, Dopp E, Pemsel H, Jonas L, Weiss DG, et al. Evidence that ultrafine titanium dioxide induces micronuclei and apoptosis in Syrian hamster embryo fibroblasts. *Environ Health Perspect* 2002;110(8):797–800.
- Sayes CM, Reed KL, Warheit DB. Assessing toxicity of fine and nanoparticles: comparing in vitro measurements to in vivo pulmonary toxicity profiles. *Toxicol Sci* 2007;97:163–80.
- Sharma HS, Hussain S, Schlager J, Ali SF, Sharma A. Influence of nanoparticles on blood-brain barrier permeability and brain edema formation in rats. *Acta Neurochir Suppl* 2010;106:359–64.
- Sharma HS, Sharma A. Nanoparticles aggravate heat stress induced cognitive deficits, blood-brain barrier disruption, edema formation and brain pathology. *Prog Brain Res* 2007;162:245–73.
- Shi H, Magaye R, Castranova V, Zhao J. Titanium dioxide nanoparticles: a review of current toxicological data. *Part Fibre Toxicol* 2013. <http://dx.doi.org/10.1186/1743-8977-10-15>.
- Shukla RK, Sharma V, Pandey AK, Singh S, Sultana S, Dhawan A. ROS-mediated genotoxicity induced by titanium dioxide nanoparticles in human epidermal cells. *Toxicol In Vitro* 2011;25:231–41.
- Sun D, Meng TT, Loong H, Hwa TJ. Removal of natural organic matter from water using a nanostructured photocatalyst coupled with filtering membrane. *Water Sci Technol* 2004;49:103–10.
- Sun Q, Tan D, Ze Y, Sang X, Liu X, Gui S, et al. Pulmotoxicological effects caused by long-term titanium dioxide nanoparticles exposure in mice. *J Hazard Mater* 2012;235–236:47–53.
- Takenaka S1, Karg E, Roth C, Schulz H, Ziesenis A, Heinemann U, et al. Pulmonary and systemic distribution of inhaled ultrafine silver particles in rats. *Environ Health Perspect* 2001;109:547–51.
- Tang M1, Zhang T, Xue Y, Wang S, Huang M, Yang Y, et al. Metabonomic studies of biochemical changes in the serum of rats, by intratracheally instilled TiO_2 nanoparticles. *J Nanosci Nanotechnol* 2011;11:3065–74.
- Tiffany-Castiglioni E, Hong S, Qian Y. Copper handling by astrocytes: insights into neurodegenerative diseases. *Int J Dev Neurosci* 2011;29:811–8.
- Valant J, Iavicoli I, Drobne D. The importance of a validated standard methodology to define in vitro toxicity of nano- TiO_2 . *Protoplasma* 2012;249:493–502.
- Valdiglesias V, Costa C, Sharma V, Kiliç G, Pásaro E, Teixeira JP, et al. Comparative study on effects of two different types of titanium dioxide nanoparticles on human neuronal cells. *Food Chem Toxicol* 2013;57:352–61.
- Vamanu CI, Cimpan MR, Høl PJ, Sørnes S, Lie SA, Gjerdet NR. Induction of cell death by TiO_2 NPs: studies on a human monoblastoid cell line. *Toxicol In Vitro* 2008a;22:1689–96.
- Vamanu CI, Høl PJ, Allouni ZE, Elsayed S, Gjerdet NR. Formation of potential titanium antigens based on protein binding to titanium dioxide nanoparticles. *Int J Nanomed* 2008b;3:69–74.
- Wang J, Chen C, Liu Y, Jiao F, Li W, Lao F, et al. Potential neurological lesion after nasal instillation of TiO_2 nanoparticles in the anatase and rutile crystal phases. *Toxicol Lett* 2008a;183(1–3):72–80.
- Wang J, Liu Y, Jiao F, Lao F, Li W, Gu Y, et al. Time-dependent translocation and potential impairment on central nervous system by intranasally instilled TiO_2 nanoparticles. *Toxicology* 2008b;254(1–2):82–90.
- Wang JX, Li YF, Zhou GQ, Li B, Jiao F, Chen CY, et al. Influence of intranasal instilled titanium dioxide nanoparticles on monoaminergic neurotransmitters of female mice at different exposure time. *Zhonghua Yu Fang Yi Xue Za Zhi* 2007;41(2):91–5.
- Warheit DB, Webb TR, Reed KL, Frerichs S, Sayes CM. Pulmonary toxicity study in rats with three forms of ultrafine- TiO_2 particles: differential responses related to surface properties. *Toxicology* 2007a;230:90–104.
- Warheit DB, Webb TR, Reed KL. Pulmonary toxicity screening studies in male rats with M5 respirable fibers and particulates. *Inhal Toxicol* 2007b;19:951–63.
- Westerink RHS. Do we really want to REACH out to in vitro? *Neurotoxicology* 2013;39:169–72. <http://dx.doi.org/10.1016/j.neuro.2013.10.001>.
- Wolf R, Matz H, Orion E, Lipozencic J. Sunscreens – the ultimate cosmetic. *Acta Dermatovenereol Croat* 2003;11:158–62.
- Wu J, Sun J, Xue Y. Involvement of JNK and P53 activation in G2/M cell cycle arrest and apoptosis induced by titanium dioxide nanoparticles in neuron cells. *Toxicol Lett* 2010;199:269–76.
- Xia T, Kovochich M, Brant J, Hotze M, Sempf J, Oberley T, et al. Comparison of the abilities of ambient and manufactured nanoparticles to induce cellular toxicity according to an oxidative stress paradigm. *Nano Lett* 2006;6:1794–807.
- XiaoBo L, ShunQing X, ZhiRen Z, Schluessener HJ. Apoptosis induced by titanium dioxide nanoparticles in cultured murine microglia N9 cells. *Chin Sci Bull* 2009;54:3830–6.
- Xie HR, Hu LS, Li GY. SH-SY5Y human neuroblastoma cell line: in vitro cell model of dopaminergic neurons in Parkinson's disease. *Chin Med J (Engl)* 2010;123(8):1086–92.
- Ze Y, Sheng L, Zhao X, Hong J, Ze X, Yu X, et al. TiO_2 nanoparticles induced hippocampal neuroinflammation in mice. *PLOS ONE* 2014a;9:e92230.
- Ze Y, Hu R, Wang X, Sang X, Ze X, Li B, et al. Neurotoxicity and gene-expressed profile in brain-injured mice caused by exposure to titanium dioxide nanoparticles. *J Biomed Mater Res A* 2014b;102:470–8.